Aerodynamic behaviour of an inclined circular cylinder

Shaohong Cheng[†]

Department of Civil Engineering, University of Ottawa, Ottawa, Ontario, Canada

Guy L. Larose[‡] and Mike G. Savage[‡]

National Research Council, Ottawa, Ontario, Canada

Hiroshi Tanaka[‡†]

Department of Civil Engineering, University of Ottawa, Ottawa, Ontario, Canada

Abstract. Galloping instability of dry inclined cables of cable-stayed bridges has been reported by Japanese researchers. A suggested stability criterion based on some experimental studies in Japan implies that many of stay cables would be expected to suffer galloping instability, which, if valid, would cause serious difficulty in the design of cable-stayed bridges. However, this is not the case in reality. Thus, it is practically urgent and necessary to confirm the validity of this criterion and possible restriction of it. In the present study, a 2D sectional cable model was tested in the wind tunnel, and effects of various physical parameters were investigated. It is found that the stability criterion suggested by Japanese researchers is more conservative than the results obtained from the current study.

Key words: cable aerodynamics; inclined circular cylinder; high-speed vortex excitation; dry inclined cable instability; Reynolds number.

1. Introduction

The inclined nature of stay cables on cable-stayed bridges introduces some new types of cable aerodynamic phenomena, i.e., rain-wind-induced cable vibration, high-speed vortex excitation, and dry inclined cable galloping. Among the three, rain-wind-induced vibration has been extensively studied since late 1980s, and the excitation mechanism is better understood so far. However, the other two types of motion, particularly the dry inclined cable galloping, still need intensive research attention, since it will result in divergent type of motion.

A limited number of studies (Saito *et al.* 1994, Miyata *et al.* 1994, Honda *et al.* 1995) have been conducted on this topic. A stability criterion based on mass-damping parameter was suggested by Saito *et al.* (1994) as

---

† Post Doctoral Research Fellow
‡ Research Officer
‡† Professor

$$(U_r)_{cr} = 14\sqrt{S_c} \qquad \qquad (1)$$

where $U_r = U/fD$ is the reduced wind speed, $S_c = m\delta/(\rho D^2)$ is the Scruton number, U is the wind speed, f is the cable frequency, D is the cable diameter, m is the cable mass per unit length, δ is the logarithmic decrement, and ρ is the air density. However, if this criterion is valid, for a typical stay cable, for example, with the diameter of 160 mm, fundamental frequency of 1.6 Hz and the linear mass density of 100 kg/m, a very large amplitude vibration would be expected at wind speed of 16 m/s, if the damping ratio is 0.1% of critical. In practice, the mechanical damping ratio of stay cables is generally less than 0.1% of critical. These numbers thus indicate that the dry inclined cable can be excited at a relatively low wind speed, even if its damping is very high. Therefore, it would easily disqualify majority of stay cables of the existing and projected cable-stayed bridges and cause serious design difficulties. The reality, however, is that many existing stay cables seem to be surviving without suffering this instability. There seem to be some limited number of cases where the claimed type of instability may explain the situation better than any other ways (Virlogeux 1998, Irwin *et al*. 1999). The possibilities are that there could be a better, refined stability criterion for inclined cable galloping, or a range of the physical parameters associated with the criterion should be more restricted.

The objective of the present study is to first confirm the existence of this type of instability. Secondly, if it indeed exists, the influence of various physical parameters on cable behavior must be identified, so that a method to eliminate or mitigate the adverse effects of the instability can be developed.

2. Wind tunnel tests

2.1. Cable model

In order to reproduce the instability of inclined dry cables identified by other researchers, a series for wind tunnel tests of a 2D sectional cable model was carried out in the wind tunnel at the Institute of Aerospace Research, National Research Council Canada (IAR/NRCC). The open circuit wind tunnel employed for the tests has a maximum wind speed of 39 m/s. The working section is 12 m long, 3 m wide and 6 m high.

The 6.7 m long full-scale cable model is a faithful reproduction of what was used in an earlier study (Saito *et al*. 1994), except the model length is a little shorter because of the size of the wind tunnel. It is made of a steel pipe wrapped by a smooth polyethylene sheet. It has a diameter of 160 mm and linear density of 60.8 kg/m.

2.2. Angle relationships

Assume that wind blows horizontally along $A'O$ with an angle β to the bridge axis, and cable is in a vertical plane AOC parallel to the bridge axis, as shown in Fig. 1 (after P. A. Irwin). The orientation of the stay cable on a cable-stayed bridge with respect to the mean wind direction can thus be represented by a horizontal yaw angle β and a vertical inclination angle θ, where β is the angle between the horizontal projection AO of the cable and wind vector $A'O$, θ is the angle between the cable axis CO and its horizontal projection AO (or the bridge axis). The cable cross-section shown in the figure is normal to the cable axis. However, what is really important, or what wind really 'sees' is the relative angle Φ between the cable and wind in the plane $A'OC$ determined by the cable axis and the
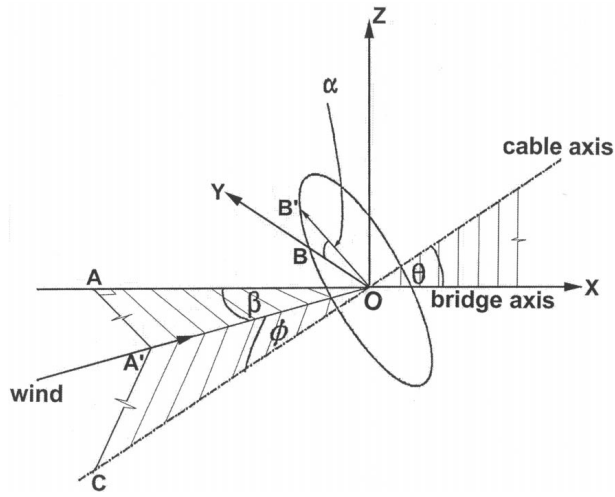
Fig. 1 Angle relations

wind vector, and the angle α indicating the predominant cable motion direction along *OB'*. Given a set of orientation angles β and θ for a bridge stay cable, the relative angles Φ and α can be determined by

$$\cos\Phi = \cos\beta\cos\theta \qquad (2)$$

$$\tan\alpha = \tan\beta/\sin\theta \qquad (3)$$

Because of the size of the cable model and the limitation in the dimension of the wind tunnel facility, the simulation of cable orientation angles, θ and β, for the range of interest is difficult to reproduce. Thus, the corresponding set of wind-cable relative angle Φ and cable motion direction angle α are considered instead in the present study.

2.3. Model setup

The two ends of the model were supported respectively on the upper and bottom part of a specially
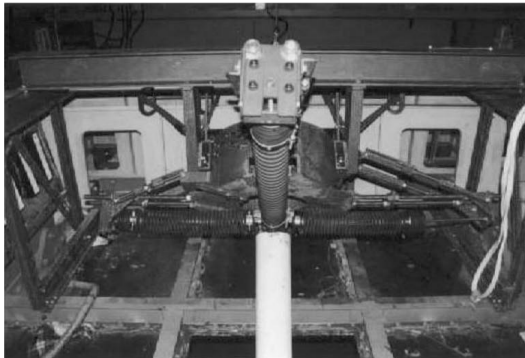
(a) Top part of the rig   (b) Bottom part of the rig
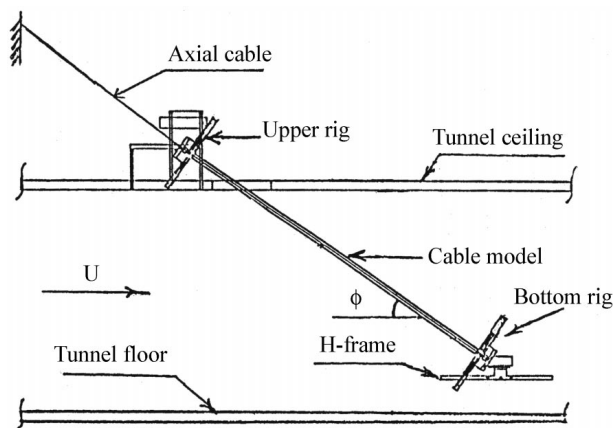
Fig. 2 Cable supporting rig

Fig. 3 Model setup

designed rig, as shown in Figs. 2 and 3. The upper part of the rig was anchored above the wind tunnel roof to minimize its influence on the upstream flow. The bottom part of the rig rested on a horizontal H-beam fixed across the tunnel section. The distance from the tunnel floor to the elevation of the beam can be adjusted to achieve different vertical setup angle Φ, which is the relative angle between the cable axis and mean wind direction. Two pairs of springs were set in the perpendicular directions on each part of the rig. Both springs were in the plane perpendicular to the cable axis and could be rotated about it. The adjustment of the spring stiffness controls the change in cable frequencies along the spring direction. An axial cable was attached to the upper end of the model to help supporting of its self-weight. The model vertical setup angle Φ and the spring rotation angle α at the two ends are adjustable to represent different combinations of inclination angle θ and yaw angle β on the real bridge cable.

The aerodynamic behaviour of the inclined cable model was investigated by different combinations of model setup, damping level and surface roughness, as described in Tables 1~3. For the initial setup, a pair of springs at each end was set along the horizontal direction, while another pair was set

Table 1 Model set-up

Model Set-up	Full-scale cable angles (deg.)		Model cable angles (deg.)	
	θ	β	Φ	α
1B	45	0	45	0
1C	30	35.3	45	54.7
2A	60	0	60	0
2C	45	45	60	54.7
3A	35	0	35	0
3B	20	29.4	35	58.7

Table 2 Different damping level

Low	No damper added
Intermediate	16 elastic bands per sway spring
High	28 elastic bands per spring for both direction
Very high	Airpot damper with 1 1/4 dial turn

Table 3 Surface condition

Smooth	Clean cable
Rough	Glue sprayed on the windward side of the cable

perpendicular to it (spring rotation angle $\Phi=0^{\circ}$). In this paper, the direction along the initial horizontal spring is defined as *X*, and *Y* is defined normal to it. This definition is kept consistent even for the cases of spring rotation angle other than 0°.

3. Characteristics of cable response

Both the divergent type of cable vibration and the limited-amplitude cable motion at certain wind speed ranges were identified during the tests.

3.1. Divergent motion

Divergent motion of the cable was observed only in Setup 2C, of which the model has a vertical angle of $\Phi=60^{\circ}$ and spring rotation angle of $\alpha=54.7^{\circ}$. This is equivalent to the full-scale cable orientation of the vertical inclination angle $\theta=45^{\circ}$ and horizontal yaw angle $\beta=45^{\circ}$.
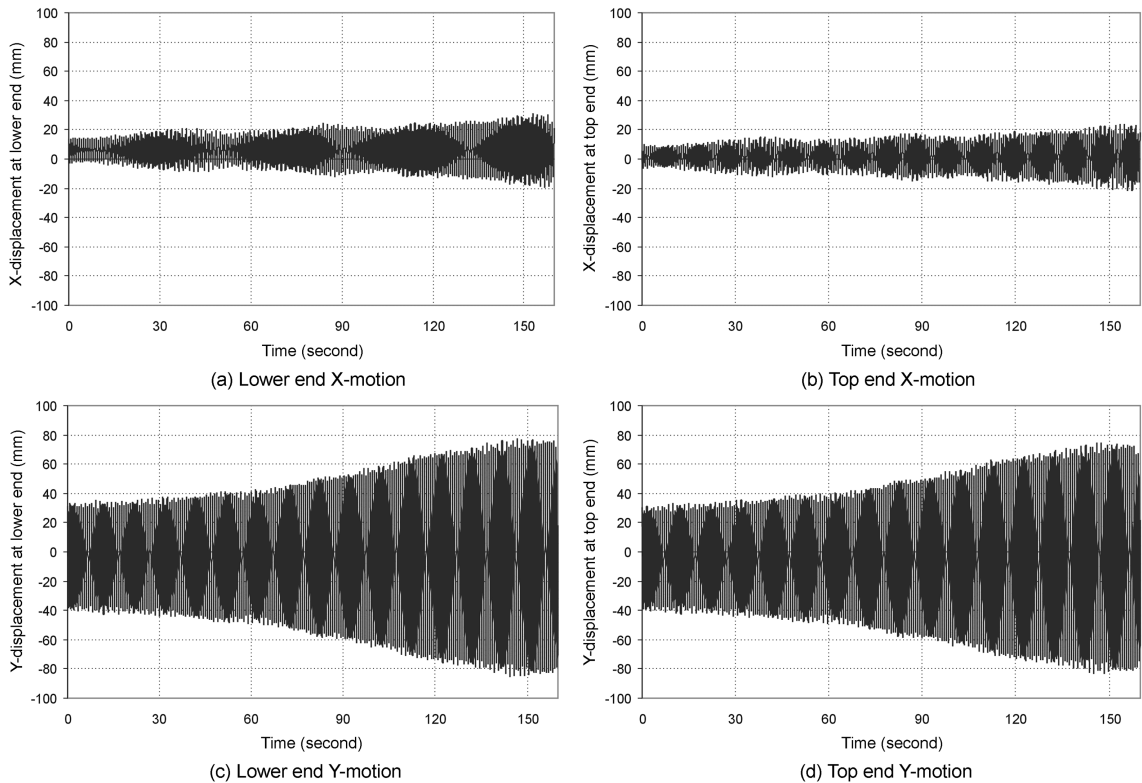

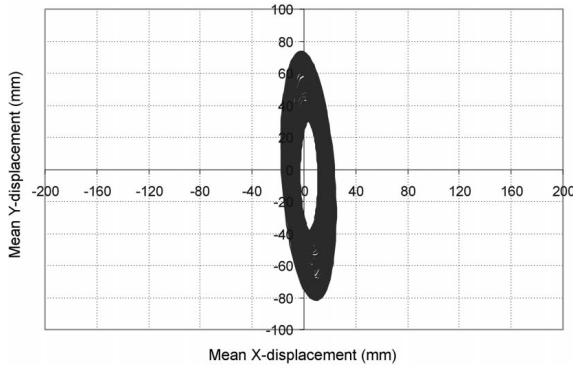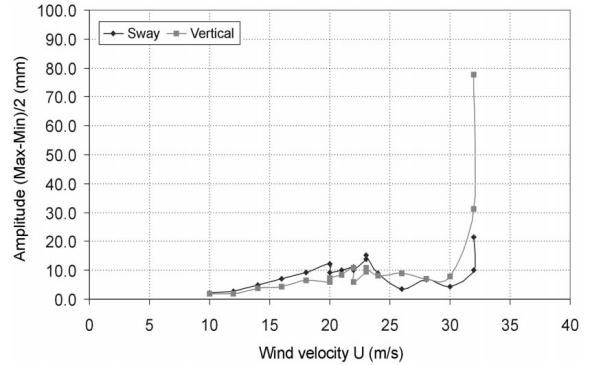Fig. 4 Time histories of cable motion in Setup 2C at $U = 32$ m/s

Fig. 5 Motion trajectory (Setup 2C, U = 32 m/s)

Fig. 6 Divergent type of response(Setup 2C, smooth surface, low damping)

The test started at a low wind speed of 10 m/s. With the increment of wind speed by 2 m/s, the amplitude of the cable motion increased slightly with the wind speed. At the wind speed of 20 m/s, the end-to-end motion was observed. This type of vibration lasted till the wind speed was increased to 23 m/s, where the motion switched to an organized harmonic type with a magnitude of ±15 mm in both X- and Y-directions. This motion was maintained with the same order of magnitude until wind speed reached 32 m/s. At this wind speed, the observed cable motion became more organized and the amplitude in Y-direction was built up steadily from ±20 mm to ±80 mm within 3 minutes. As shown in Figs. 4 and 5, which are the time histories of cable motion along X-and Y-directions at both model ends and the motion trajectory, the predominant motion occurred in Y-direction, and the model followed an elliptical path. The motion looked to have the tendency of growing further, but it had to be manually suppressed because of the limited model setup clearance at the wind tunnel ceiling. The recorded peak-to-peak amplitude was about 1D, where D is the cable diameter. Fig. 6 shows the wind-induced response of the model in Setup 2C.

3.2. Limited-amplitude motion

The limited-amplitude motion of the inclined cable model was observed at certain wind speed ranges for the Setups 2A, 1B, 1C and 3A. The maximum amplitude, the wind speed range of observed motion, and the corresponding Reynolds number for each individual case are given in Table 4. The ranges of unstable behaviour are clearly shown in the response curves in Figs. 7-10. Based on the observed phenomena, this limited-amplitude cable motion looks more like vortex shedding rather than galloping. The characteristics of the motion are summarized as follows:

Table 4 Limited-amplitude motion

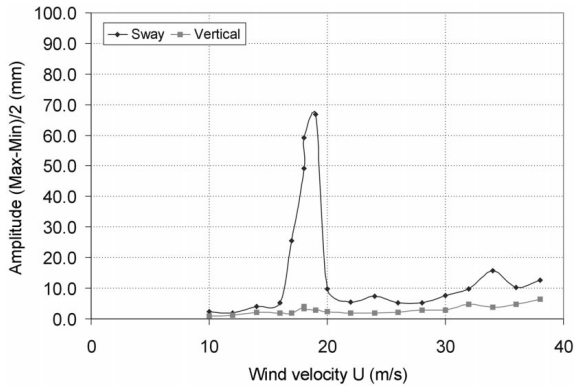| Model Setup	Unstable range				
	U (m/s)	U_r	Max. Amp. (mm)	$R_e = UD/\nu$	$S_c = m\delta/(\rho D^2)$
2A	18-19	79-84	67	1.86~1.96×10^5	11.0
1B	24-26	106-114	31	2.48~2.68×10^5	7.7
1C	34-38	150-167	25	3.51~3.92×10^5	10.0
3A	22	96	20	2.27×10^5	8.8

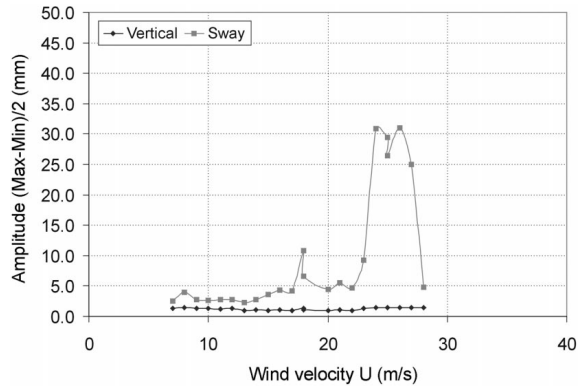Fig. 7 Limited-amplitude response(Setup 2A, smooth surface, low damping)

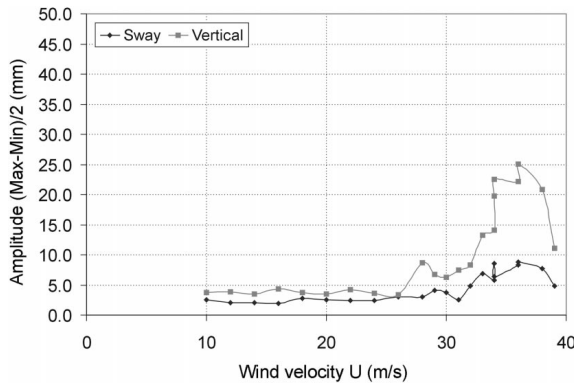Fig. 8 Limited-amplitude response(Setup 1B, smooth surface, low damping)

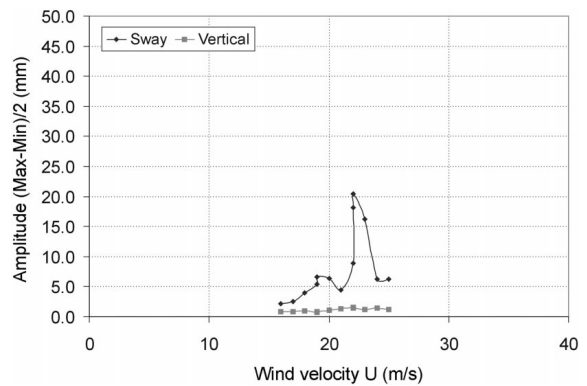Fig. 9 Limited-amplitude response(Setup 1C, smooth surface, low damping)

Fig. 10 Limited-amplitude response(Setup 3A, smooth surface, low damping)

3.2.1. Amplitude

The amplitude of the motion is limited. As given in Table 4, the largest amplitude observed was in Setup 2A. When wind velocity is 19 m/s, the amplitude of the cable motion reached 67 mm, which is about 0.42D, where D is the cable diameter.

The maximum magnitude of the unstable motion depends on the orientation angle of the cable. It was larger with a greater vertical inclination angle. In Setup 3B, which represents the full-scale cable with a very shallow inclination angle of 20° and yaw angle of 29.4^o, no unstable motion was observed within the wind speed range of 8 m/s -34 m/s. Fig. 11 shows the response curve in the tested wind speed range with Setup 3B. It can be seen that the amplitude of the motion remained less than 5 mm.

3.2.2. Wind velocity

The large amplitude motion was observed only in the limited wind velocity range, but at different
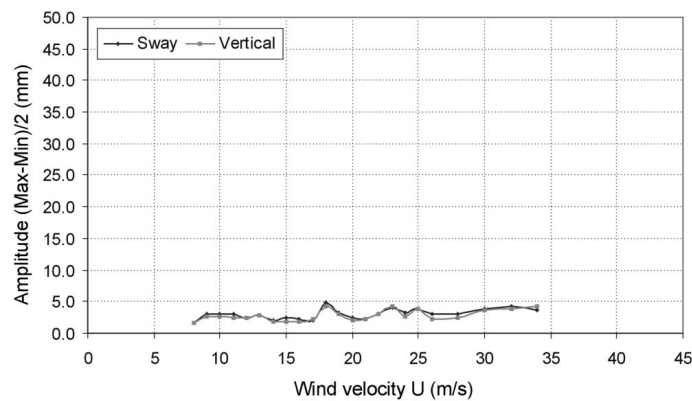
Fig. 11 Limited-amplitude response (Setup 3B, smooth surface, low damping)

wind speed levels corresponding to different setups. The reduced wind velocities corresponding to these ranges are approximately the multiples of 20.

3.2.3. Reynolds number

The critical Reynolds number corresponding to sudden decrease of the drag force is influenced by both surface roughness of the cable and flow turbulence. The critical Reynolds number for a smooth circular cylinder in uniform flow is $2 \sim 4 \times 10^5$. It is interesting to find that all of these unstable behaviour observed in the current tests occurred more or less at the wind speed corresponding to this critical Reynolds number range.

3.2.4. Response characteristics

There were two types of response: a very organized harmonic motion, and a motion with regular beating, which is similar to what Matsumoto (1998) described as the case of 3D Karman vortex shedding. According to Matsumoto, this regular beating is caused by the fluid interaction between the axial vortices along the inclined cable surface and the Karman vortices in the wake of the cable. The Karman vortex shedding is said to be amplified intermittently by the axially produced vortices and induces the beating type of motion.

In some of the setups when the spring rotation angle is not 0°, which is equivalent to wind horizontally skewed to the cable in practice, an elliptical motion of the cable was observed, which corresponds well with the field observations (Matsumoto *et al*. 1990).

4. Parametric study

4.1. Damping effect

The observed unstable cable motion is likely to be influenced by both of its mass and damping. However, the use of the Scruton number, which is a dimensionless product of these two different parameters, as a single parameter to define the instability criterion as suggested by the previous

study (Saito *et al.* 1994) may not be reasonable. There is no reason why the damping and mass should have the same effect on this dynamic behaviour, and thus these two effects should be investigated separately. It is necessary to clarify the required magnitude of structural damping to control this type of instability to a harmless level.

The behaviour of the inclined cable model under four different levels of structural damping, i.e., low, intermediate, high, and very high levels, as described in Table 2, were tested in Setup 1B. The relationship between the critical damping ratio and the sway amplitude for these four levels of damping are given in Fig. 12. For an amplitude of typically 10 mm, these four damping levels correspond to 0.03%, 0.06%, 0.24%, and 0.60% of critical. The magnitude of structural damping was controlled by applying rubber band and pneumatic dampers.

Fig. 13 shows the wind-induced response of the cable model in Setup 1B under those four levels of damping. As clearly shown in the figure, when the damping was increased, the response was significantly reduced, but the wind speed range within which the unstable behaviour was identified did not change. This set of results indicates that limited-amplitude motion can be relatively easily suppressed by increasing the damping of the cable.
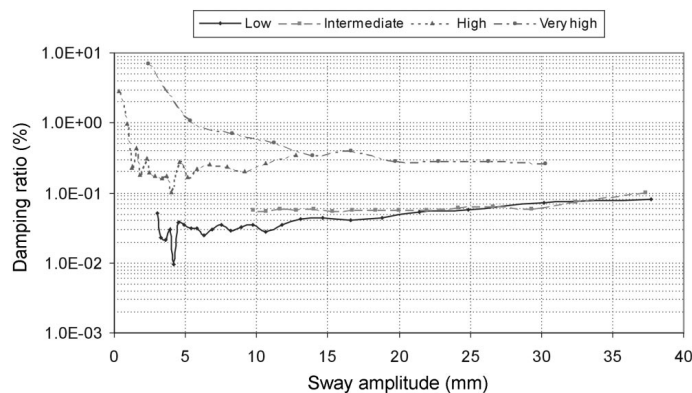

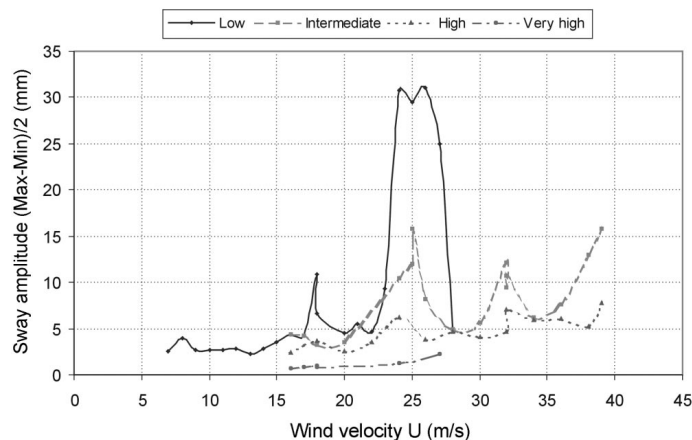Fig. 12 Damping ratio-amplitude relation (Setup 1B, smooth surface)

Fig. 13 Damping effect on the response (Setup 1B, smooth surface)

4.2. Surface roughness effect

The cable model was tested under both smooth and rough model surface conditions. For the rough surface case, a kind of liquid glue was sprayed on the windward side of the model to simulate the accumulation of dirt and salt on the real cable. Figs. 14-16 describe the response of the cable model in Setups 3A, 1B and 2A under both smooth and rough surface conditions. These three cases are equivalent to wind blowing along the cable in full-scale situation with the vertical inclination angle θ of 35°, 45° and 60°, respectively.

It can be seen from these three figures that for Setups 3A and 1B, of which the inclination angle $\theta \leq 45^{\circ}$, the increase of cable surface roughness made the unstable response range shift to lower wind speed. For Setup 2A, there were two peaks in the sway response curve of the smooth surface case: one at around 19 m/s, and another at about 34 m/s. However, in the rough surface case, only one peak was identified in the range of 31-32 m/s. No shift of wind speed range was found for this setup. Since the inclination angles of these three setups are different, the differences in the response
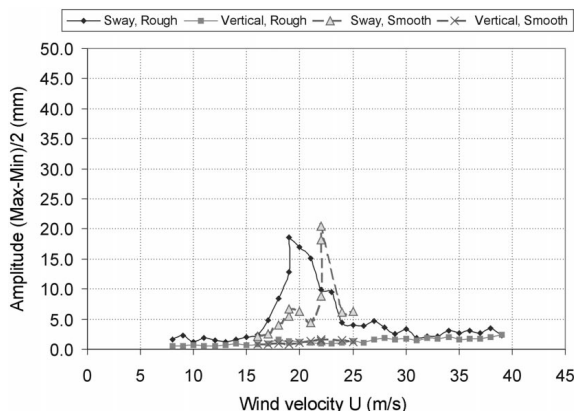

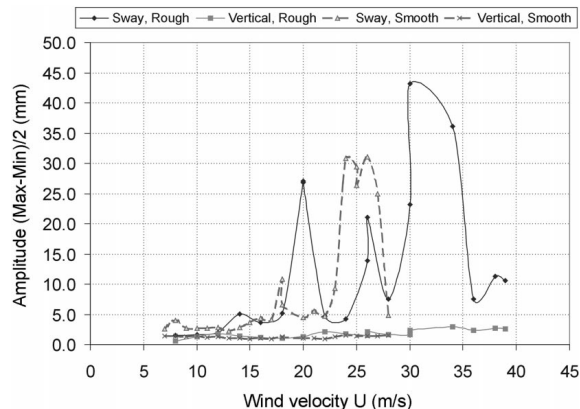Fig. 14 Surface roughness effect (Setup 3A, low damping)

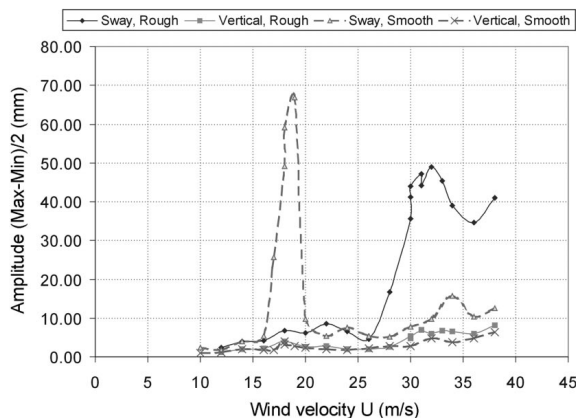Fig. 15 Surface roughness effect (Setup 1B, low damping)

Fig. 16 Surface roughness effect (Setup 2A, low damping)

given by those three figures include not only the surface roughness effect but also the influence of the cable orientation. Therefore, although the increase of cable surface roughness made the unstable response range shift to lower wind speed for the cases of $\theta \leq 45^{o}$, the effect of surface roughness in general is still inconclusive from the present study alone.

The difference of surface roughness would affect the flow separation point, which will change the critical Reynolds number. This is likely to alter the lift and drag forces acting on the cable, and thus changes its aerodynamic behaviour. Further, recent study by Larose & Zan (2001) shows that the change of orientation angle of a smooth cylinder will also affect the Reynolds number. In order to better understand the mechanism of the unstable motion of the inclined cable and develop methods to eliminate or mitigate the instability, it is very important to further explore this Reynolds number effect.

5. Comparison with other studies

A limited number of experimental studies on inclined cables have been carried out particularly in Japan. Saito *et al.* (1994) defined an instability criterion for the inclined cable motion based on three different model setups. Two of them are exactly identical to Setups 1B and 2A in the current study. Miyata *et al.* (1994) investigated the inclined dry cable motion with a configuration corresponding to Setup 2C of the present study, and identified that divergent type of motion occurs at reduced wind speed of 80. The corresponding Scruton number of the model is 2. In the study carried out by Honda *et al.* (1995), the model was placed in the horizontal plane. Its behaviour under yaw angles of 45° and 60° were tested. These correspond to the current Setups 1B and 2A, respectively. A formula describing the relation between the critical reduced wind velocity indicating the onset of instability and Scruton number was presented.

The result of the present study and these three sets of earlier work are shown together in Fig. 17. Among the results from current findings, only the one corresponding to Setup 2C is the divergent galloping motion, whereas the others are identified to be limited-amplitude, high-speed vortex shedding excitation. The Scruton number is defined as $S_c = m\delta/(\rho D^2)$ in the figure, where m is the cable mass per unit length, δ is the logarithmic decrement, ρ is the air density, and D is the cable diameter.

As it can be seen from the figure, the results obtained in the current study are concentrated in the low Scruton number range, whereas those from Saito *et al.* (1994) and Honda *et al.* (1995) cover wider range. Within the low Scruton number range of $S_c \leq 20$, present test results are found to be least conservative. Data from Honda *et al.* (1995) split into two branches, with one falling in the
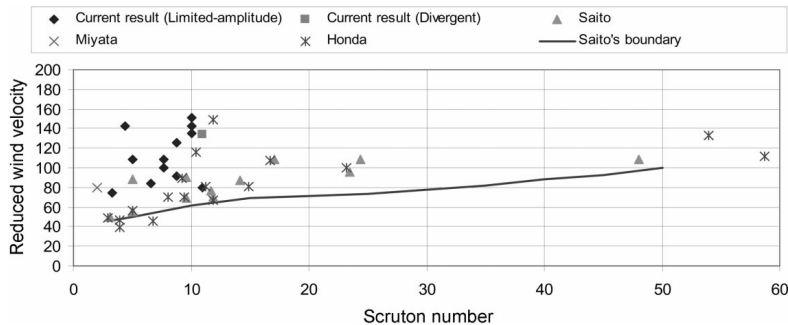

Fig. 17 Comparison of wind velocity-damping relation of inclined cable

range of the current findings, and another agrees more with Saito's results. The criterion to indicate the onset of instability defined by Saito *et al*. (1994) is much more conservative, when compared with the results given by Miyata *et al*. (1994) and the current study. Further to this, the similar instability criterion that could be defined by current findings would have much steeper slope than that given by Saito, which implies that with the increase of the cable structural damping, the instability range of the inclined cable motion will be shifted to even higher wind speed level.

6. Conclusions

A series of wind tunnel tests was conducted to investigate the aerodynamic behaviour of the inclined dry cable. Both the divergent galloping motion and the limited-amplitude high-speed vortex shedding excitation were observed. Galloping instability, which grows into a large amplitude motion, was observed in only one case. Parametric study shows that the vortex excitation can be relatively easily suppressed with the increase of structural damping. Also, if wind blows along the cable, for cables with a vertical inclination angle $\theta \leq 45^{o}$, the increase of surface roughness makes the unstable range shift to lower wind speeds. The instability criterion for inclined cable vibration defined by Saito is found to be more conservative than the results obtained from the current study. The Reynolds number effect, which is resulted from the model surface condition and the orientation angle, needs to be further explored.

Acknowledgements

References

Honda, A., Yamanaka, T., Fujiwara, T. and Saito, T. (1995), "Wind tunnel test on rain-induced vibration of the stay-cable", *International Symposium on Cable Dynamics*, Liege, Belgium, 255-262.
Irwin, P.A., Nedim, A. and Telang, N. (1999), "Wind induced stay cable vibrations - A case study", *Proceedings of 3rd International Symposium on Cable Aerodynamics*, Trondheim, Norway, 171-176.
Irwin, P.A., "Angle relationships for cables and wind on cable-stayed bridges", *Personal communication.*
Larose, G.L. and Zan, S.J. (2001), "The aerodynamic forces on the stay cables of cable-stayed bridges in the critical Reynolds number range", *Proceedings of 4th International Symposium on Cable Aerodynamics*, Montreal, 77-84.
Matsumoto, M. (1998), "Observed behaviour of prototype cable vibration and its generation mechanism", *Bridge Aerodynamics*, Larsen & Esdahl (eds), Balkema, Rotterdam, 189-211.
Matsumoto, M., Shiraishi, N., Kitazawa, M., Knisely, C., Shirato, H., Kim, Y. and Tsujii, M. (1990), "Aerodynamic behaviour of inclined circular cylinders-cable aerodynamics", *J. Wind Eng. Ind. Aerod.*, **33**, 63-72.
Miyata, T., Yamada, H. and Hojo, T. (1994), "Aerodynamic response of PE stay cables with pattern-indented surface", *Proceedings of the International Conference on Cable-stayed and Suspension Bridges (AFPC)*, Deauville, **2**, 515-522.
Saito, T., Matsumoto, M. and Kitazawa, M. (1994), "Rain-wind excitation of cables on cable-stayed Higashi-Kobe Bridge and cable vibration control", *Proceedings of the International Conference on Cable-stayed and Suspension Bridges (AFPC)*, Deauville, **2**, 507-514.
Virlogeux, M. (1998), "Cable vibrations in cable-stayed bridges", *Bridge Aerodynamics*, Larsen & Esdahl (eds), Balkema, Rotterdam, 213-233.

CC